8. The Synchronous Machine

8.1 Principle of Operation and Rotor Design

a) The Rotor Rotates Synchronously with the Stator Field:

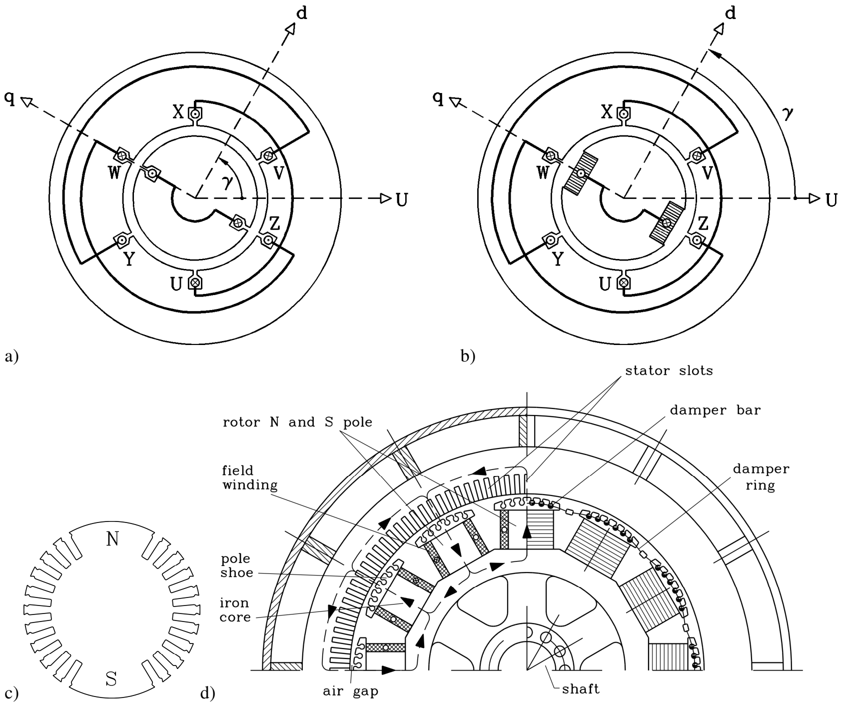

Fig. 8.1: Designs of synchronous machines: a) sketch of a round-rotor machine ($2p = 2$, $m_s = 3$, $q_s = 1$, $m_r = 1$, $q_r = 1$) b) salient-pole machine (parameters as a)), c) axial cross section of a two pole round-rotor machine d) 12-pole salient-pole machine

The slotted stator with three-phase winding as explained in Chapter 2 is combined with a rotor that generates a magnetic field by itself e.g. by permanent magnets or coils that are excited by a dc current. Thus, a **synchronous machine** is obtained. If the stator winding is connected to the three-phase line, a stator rotating field is generated. This field interacts with the rotor magnetic field, thereby “dragging” the rotor **synchronously** with the stator field (**motor operation**), the slip is always zero. If – on the contrary – the rotor is driven e.g. by a turbine and the stator winding is at zero current, the rotating rotor field causes an alternating flux linkage in the stator winding. Thereby, a voltage with a frequency that corresponds to the product of the frequency of rotation and the number of poles of the machine is induced in the stator winding.

$$f_s = n \cdot p \qquad (8.1)$$

If a load is applied e.g. by connection of external resistors to the stator winding, current flows in the stator winding and mechanical energy is converted into electrical energy (**generator**

operation). The rotating stator field, generated by the stator currents, rotates due to the above mentioned frequency of the stator voltages and currents synchronously with the rotor at **synchronous speed**.

$$\boxed{n = n_{syn} \quad \Rightarrow \quad \Omega_m = 2\pi \frac{f_s}{p} = \Omega_{syn}} \qquad (8.2)$$

b) The Rotor Is Either Excited By Permanent Magnets or Is Electrically Excited:

Small synchronous machines are often designed with permanent magnet rotors, notably as synchronous servo motors. In the case of an electrically excited synchronous machine, the rotor magnetic field is excited by a dc coil arrangement with the required numbers of poles. Generally, this dc-current is supplied to the rotor via sliprings. When compared with permanent magnet machines, this technique offers the advantage of an additional degree of freedom concerning the setting of the operating point of a machine, because the rotor field can be varied during operation. Electrically excited synchronous machines are notably used as generators, because the **variable excitation** of the rotor allows to meet **any demands of the power factor** $\cos\varphi$ (capacitive or inductive) of the line.

Please note: This is not possible with **asynchronous generators** which always require some magnetising current, thereby always consuming inductive reactive power.

c) Round-Rotor Machine:

Two types of electrically excited rotors are distinguished:

Round-rotor machines:

The field coils of the cylindrical rotor are distributed in slots – similar to those of the three phases of the stator winding (Fig. 8.1a, c).

Salient-pole machine:

Each of the distinctive rotor poles carries a concentric coil (Fig. 8.1b, d).

At high rotational speed, the centrifugal force on the rotor can be handled better with a round-rotor. At the same stator frequency f_s, the speed n is maximum in the case of a two-pole machine. Therefore, two-pole and often also four-pole machines are designed as round-rotor machines.

The turbo generator is a **special type** of a round-rotor machine. It has a cylindrical rotor (**“rotor body”**) from massive steel. As the rotor carries dc flux, no harmful eddy currents are induced there, and no lamination of the rotor is necessary. Massive rotors have a higher mechanical strength than laminated rotors, but the manufacturing of the slotting (via milling) is more difficult than in the case of a laminated rotor (via punching of the slots into the lamination sheets). Therefore, **round-rotors** are built as **massive rotors** (turbo rotor) if the demands on mechanical strength due to high centrifugal forces are very high. Such machines are used in **thermal power plants**, where the machine and the high-speed turbine (**steam or gas turbine**) are directly coupled at a speed of 3000/min or 3600/min (therefore the name **“turbo generator”**).

If the electric load and hence the braking stator field is switched off due to a line fault, the turbine accelerates (**“runaway” of the turbo drive**) until the speed monitoring responds and “cuts off” the steam jet, that feeds the steam turbine. This is possible using a mechanical valve within a very short time. Therefore, thermal turbo machines and turbo generators have to be designed mechanically to sustain only 20 % over-speed which corresponds to $1.2^2 = 1.44$ times the centrifugal strain when compared with rated operation. Even with the use of modern special alloyed steel with high strain limit for the massive rotor body of a turbo generator, the diameter of the rotor is limited to about 1.2 m - 1.3 m, corresponding to a maximum **“runaway” circumferential speed** of

$$v_{\max} = 1.2 \cdot d_r \pi n_{syn} = 1.2 \cdot d_r \pi (f_s / p) = 1.2 \cdot 1.3 \pi (50/1) = 245 \text{ m/s} = 880 \text{ km/h} \quad . \tag{8.3}$$

Higher circumferential speed is not possible, because the permissible tensile stress in the rotor teeth is exceeded. Therefore, 2 pole turbo generators are limited for mechanical reasons to power ratings up to 1000 MW. Details on the design of large synchronous machines are given in the lecture *"Large Generators and High Power Drives"*.

Example 8.1-1:
Turbo generator, rating: 930 MW, $\cos\varphi = 0.8$ overexcited, $U_N = 27$ kV, $I_N = 24.9$ kA
$2p = 2$, $n_N = 3000$/min, $f_N = 50$ Hz, efficiency 99%, total length of the rotor about 14 m. Direct cooling of the conductors: Deionised water flows in the hollow conductors of the stator three-phase winding. Hydrogen gas flows in the hollow conductors of the rotor field excitation conductors.

d) Salient-Pole Machines:
The poles of salient-pole rotors are either screwed to the rotor or wedged in the case of high centrifugal forces where dovetail or T-head poles are used. Large salient-pole machines are notably used as generators.
Hydropower generators are directly coupled to the water turbine.
- *PELTON* turbines of high pressure hydropower plants typically rotate with up to 1000/min. Therefore, the minimum number of poles at 50 Hz is 6.
- *FRANCIS* turbines of medium pressure power plants turn slower (e.g. 500/min) and require machines with a higher number of poles (e.g. $2p = 12$).
- In low pressure power plants, such as run-of-river power station at rivers with small head (height of fall) and high flow rate per turbine, slowly running ***KAPLAN* turbines** are used. The efficiency of these turbines can be kept at its maximum via adjustment of the rotor blades. E.g. at 100/min, a generator with 60 poles is needed to induce 50 Hz voltages.
In the case of switching off of the electric load, the water in the turbine cannot be slowed down as fast as the steam jet of the turbo groups. So the turbine accelerates up to its no-load speed. Theoretically, *PELTON* turbines can run up to twice rated speed. In reality, the speed is limited to about 1.8 n_N due to turbine losses. *FRANCIS* and *KAPLAN* turbines may even run up to about 3.5 n_N. So, the salient-poles have to be designed for that high centrifugal force.

Example 8.1-2:
High pressure power plant ***Bieudron/Switzerland***: 1.88 km (!) head from the reservoir (*Grand Dixence Dam*) down to the power station in the *Wallis* valley (today world record).
- most powerful *PELTON* turbines of the world: 423 MW
- 3 generator turbine units, each consisting of a *PELTON* turbine with five water jets and a salient-pole synchronous generator per unit.
- Generator parameters: $2p = 14$, $n_N = 428.6$/min, 50 Hz, 21 kV, 465 MVA, 12.78 kA, $\cos\varphi_N = 0.84$ overexcited, runaway speed: 800/min, stator: 281 tons, rotor: 454 tons.
- 33.2 MVA apparent power per pole (world record)
- stator and rotor winding: direct cooling with de-ionised water in the hollow conductors

8.2 Stator Equivalent Circuit of a Round-Rotor Machine

a) Magnetic Fields and Flux Linkages
Fig. 8.2 shows a simplified axial cross section of a two-pole round-rotor synchronous machine. The unrolled rotor is shown in Fig. 8.3 with stator slotting neglected. 2/3 of the rotor circumference is slotted. The pole flux flows via the unslotted third of each pole pitch. In Fig. 8.3, 8 out of 12 possible slots per pole pair are used, 4 slots per pole, containing the

conductor including the returns of the rotor coils. Each slot contains a coil with N_{fc} turns. Hence, if all coils are connected in series, the ampere-turns per slot are $N_{fc}I_f$. When compared with a three phase winding (Chapter 2), it is obvious that the distributed field winding generates the same magnetic voltage $V_f(x)$ as a single phase of a dc fed three phase winding with $W/\tau_p = 2/3$. In the example of Fig. 8.3, the number of slots per pole and phase is $q_r = 2$. Due to series connection of all coils, the number of windings per phase is

$$N_f = 2p \cdot q_r \cdot N_{fc} = 2p \cdot N_{fPol} \quad . \tag{8.4}$$

The m.m.f. distribution $V_f(x)$ is at rest when seen from the rotor, because it is excited by a dc current. The amplitude of the fundamental of the flux distribution $\mu = 1$ of the field winding can be expressed by the *FOURIER* analysis of the m.m.f. distribution of a single phase of a three phase winding (Chapter 3):

$$\hat{V}_f = \frac{2}{\pi} \cdot \frac{N_f}{p} \cdot k_{w,f} \cdot I_f \tag{8.5}$$

$$k_{w,f} = k_{p,f} k_{d,f}\, , \quad k_{p,f} = \sin\left(\frac{W}{\tau_p} \cdot \frac{\pi}{2}\right) = \sin(\pi/3) = \frac{\sqrt{3}}{2}\, , \quad k_{d,f} = \frac{\sin(\pi/6)}{q_r \sin(\pi/(6q_r))} \tag{8.6}$$

At $\mu_{Fe} \to \infty$, the **amplitude of the fundamental** $\mu = 1$ of the rotor field is given by (8.7).

$$\hat{B}_p = \mu_0 \frac{\hat{V}_f}{\delta} \tag{8.7}$$

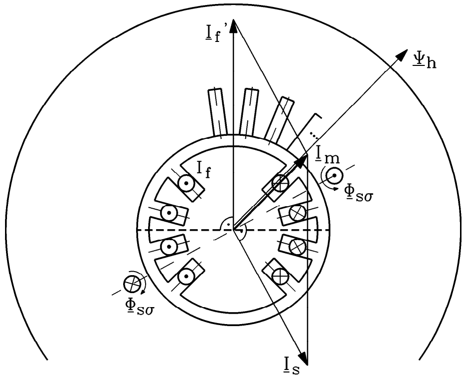

Fig. 8.2: Sketch of axial cross section of a round-rotor synchronous machine with excited stator and rotor winding and corresponding current and flux linkage phasors $\underline{I}_s$, $\underline{I}'_f$, $\underline{I}_m$ and $\underline{\Psi}_h$.

The sinusoidal field B_p induces a three-phase system of rotating voltages in the three-phase stator winding (**"synchronous generated voltage or back e.m.f."**) with an r.m.s.-value of

$$U_p = \omega \cdot \Psi_p / \sqrt{2} = \omega \cdot N_s k_{w,s} \cdot \Phi_p / \sqrt{2} = \sqrt{2}\pi f \cdot N_s k_{w,s} \cdot \frac{2}{\pi} l \tau_p \hat{B}_p \tag{8.8}$$

and the frequency given by (8.9) as the rotor rotates at speed n.

$$\boxed{f = n \cdot p} \tag{8.9}$$

At open stator winding terminals and externally driven, excited rotor, this voltage can be measured at the stator terminals (**"no-load test"**).

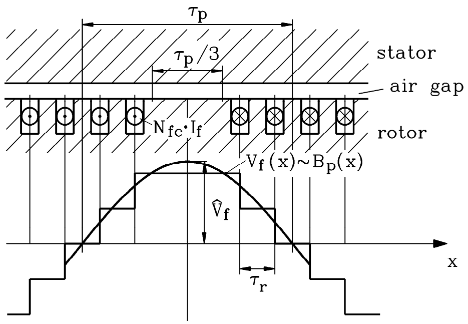

Fig. 8.3: Linearly unrolled round-rotor machine with excited rotor (field current I_f) and corresponding m.m.f. distribution $V_f(x)$ including the *FOURIER* fundamental

The harmonics of the stator field distribution $B_p(x)$ induce the stator winding as well. These voltages with higher frequencies are parasitic effects and are kept as small as possible by appropriate short-pitching of the stator winding. Hence, the stator voltage is almost sinusoidal in spite of the step like rotor field distribution. So, only the fundamental of the rotor field distribution is considered in the following.

In the reverse case, if the rotor is at zero current and the stator winding is fed with a three phase current I_s with the frequency f_s, a rotating step-like distribution of the m.m.f. $V_s(x)$ with a fundamental amplitude $\hat{V}_s$ is generated (Chapter 3).

$$\hat{V}_s = \frac{\sqrt{2}}{\pi} \cdot \frac{m_s}{p} \cdot N_s k_{w,s} \cdot I_s \quad \Rightarrow \quad \hat{B}_s = \mu_0 \frac{\hat{V}_s}{\delta} \quad . \tag{8.10}$$

This amplitude excites a magnetic field fundamental B_s, rotating with $\Omega_{syn} = 2\pi f_s / p = \omega_s / p$ and causing self-induction voltage $\omega_s L_h I_s$ in the stator winding. The rotor, moving synchronously with this field ($n = n_{syn} = f_s / p$), is **not** induced by this stator rotating field, because in the rotor the stator flux linkage does NOT change. Rotor and stator rotating field are **at rest relatively to each other**.

Fig. 8.2 shows a **general operating state** where both the rotor field winding and the stator winding carry current. As the fundamental of the rotor and the stator flux linkage are both spatially sinusoidally distributed and are at rest relative to each other, they may be added. Together, they give an overall m.m.f. $V_m(x)$ that is again sinusoidally distributed. Spatial sinusoidally distributed magnetic fields and magnetic voltages in the air gap are described by **space vectors** (Chapter 5), where the vector length indicates the amplitude and the vector direction indicates the orientation of the north pole (Fig. 8.2). **Instead of the vector of the stator m.m.f.** $\hat{V}_s$, the stator current phasor I_s itself is used (8.10), and instead of the vector of the rotor m.m.f. $\hat{V}_f$, the **equivalent field current** I'_f is used (8.11).

$$I'_f = \hat{V}_f \cdot \frac{I_s}{\hat{V}_s} = \frac{2 N_f k_{w,f}}{m_s N_s k_{w,s} \sqrt{2}} I_f = \frac{1}{\ddot{u}_{If}} I_f \tag{8.11}$$

The sum $\underline{I}_s + \underline{I}'_f$ is the phasor of the **"magnetising current"** $\underline{I}_m$, corresponding to the amplitude of m.m.f. $\hat{V}_m$ that excites the resultant air gap rotating field with the amplitude $\hat{B}_h$. The influence of iron saturation is neglected.

$$\underline{I}_m = \underline{I}_s + \underline{I}'_f \tag{8.12}$$

$$\hat{V}_m = \frac{\sqrt{2}}{\pi} \cdot \frac{m_s}{p} \cdot N_s k_{w,s} \cdot I_m \tag{8.13}$$

$$\hat{B}_h = \mu_0 \cdot \hat{V}_m / \delta \tag{8.14}$$

b) Voltage Induction:

The main flux linkage per phase of the stator winding Ψ_h pulsates with frequency f_s and induces the **internal voltage** U_h (= **induced voltage** U_i) per phase in the stator winding.

$$\Psi_h = N_s k_{w,s} \cdot \Phi_h = N_s k_{w,s} \cdot \frac{2}{\pi} \tau_p l \hat{B}_h \tag{8.15}$$

$$U_h = \omega_s \cdot \Psi_h / \sqrt{2} = \omega_s \cdot N_s k_{w,s} \cdot \Phi_h / \sqrt{2} = \sqrt{2}\pi f_s \cdot N_s k_{w,s} \cdot \frac{2}{\pi} l \tau_p \hat{B}_h \tag{8.16}$$

The fictive current I_m can be understood as AC current per phase in the stator winding, which excites the main field B_h that induces the internal voltage $\underline{U}_h$ by self-induction (Fig. 8.4a), where L_h is given by (8.18) according to Chapter 4.

$$\underline{U}_h = j\omega_s \underline{\Psi}_h / \sqrt{2} = j\omega_s L_h \underline{I}_m \tag{8.17}$$

$$L_h = \mu_0 N_s^2 k_{ws}^2 \frac{2 m_s}{\pi^2} \frac{l \tau_p}{p \cdot \delta}$$

The fictive AC current I'_f can be understood as that stator current, which excites the air gap field B_p that induces $\underline{U}_p$. So in equivalent circuit Fig. 8.4a a current source $\underline{I}'_f$ is used. As a result, the internal voltage $\underline{U}_h$ is given by (8.19), depending on magnetizing current $\underline{I}_m$.

$$\underline{U}_p = j\omega_s \underline{\Psi}_p / \sqrt{2} = j\omega_s L_h \underline{I}'_f \tag{8.18}$$

$$\underline{U}_h = j\omega_s L_h \underline{I}_m = j\omega_s L_h (\underline{I}_s + \underline{I}'_f) = j\omega_s L_h \underline{I}_s + \underline{U}_p \, . \tag{8.19}$$

Hence, Fig. 8.2 may be regarded a time phasor diagram of the currents $\underline{I}_s$, $\underline{I}_f'$, $\underline{I}_m$. The stator phase current I_s also excites a leakage flux $\Phi_{s\sigma}$ in the slots and in the winding overhang (Fig. 8.2) that induces the leakage voltage $\omega_s L_{s\sigma} I_s$ in the winding phases by self-induction. Taking into account the *OHM*ic voltage drop per phase, the stator phase voltage at the winding terminals U_s is obtained:

$$\underline{U}_s = \underline{U}_p + j\omega_s L_h \underline{I}_s + j\omega_s L_{s\sigma} \underline{I}_s + R_s \underline{I}_s = \underline{U}_p + jX_h \underline{I}_s + jX_{s\sigma} \underline{I}_s + R_s \underline{I}_s$$

$$\boxed{\underline{U}_s = \underline{U}_p + jX_d \underline{I}_s + R_s \underline{I}_s} \tag{8.20}$$

The back-e.m.f. U_p is a voltage source in the alternative **equivalent circuit per phase** (Fig. 8.4b), whereas the magnetising inductance X_h, the leakage inductance $X_{s\sigma}$ and the stator resistance R_s are "internal impedances" of the synchronous machine. The sum of magnetising and the leakage reactance is called **"synchronous reactance"** X_d.

$$\boxed{X_d = X_{s\sigma} + X_h} \tag{8.21}$$

c) Overexcited and Underexcited Operation:

As the consumer reference frame is used, the current is leading with respect to the voltage in Fig. 8.5 and the phase angle φ is negative; the machine acts as **a generator and as a capacitive load**, because the electric reactive power (8.22) is negative.

$$Q = m_s U_s I_s \sin\varphi \tag{8.22}$$

According to the phasor diagram, this is only possible because U_p is **significantly larger** than U_s. This requires a large excitation field, hence a large field current. Therefore, I'_f is significantly larger than I_s. This operation is called **overexcited operation**. It is defined as follows:

$Q < 0$: **"overexcited"** synchronous machine, the machine is a capacitive load
$Q > 0$: **"underexcited"** synchronous machine, the machine is an inductive load.

The real power (8.23) is also negative, because $-\pi/2 > \varphi > -\pi$ is also negative in Fig. 8.5.

$$P_e = m_s U_s I_s \cos\varphi \tag{8.23}$$

The machine acts as a generator: It delivers electric power.

$P_e < 0$: synchronous machine is **generator**,
$P_e > 0$: synchronous machine is **motor**.

The main rotor axis is called ***d*-axis** (Fig. 8.6). It is the direction of the rotor field B_p and therefore of the field current phasor $\underline{I}'_f$ in the phasor diagram. The angle between back e.m.f. and stator voltage $\underline{U}_p$ and $\underline{U}_s$ is called **load angle ϑ**. It is an indicator for the load of a synchronous machine. It is measured in electrical degrees, hence, 180° load angle corresponds to a rotor displacement of one pole pitch.

At **generator operation**, the back e.m.f. phasor $\underline{U}_p$ is leading with respect to the stator voltage phasor $\underline{U}_s$ in mathematically positive direction (Fig. 8.5). In this case, the load angle ϑ is counted **positive**. Physically, this means that the rotor is leading the air gap field, because the phasor of $\underline{I}'_f$ is ahead of the phasor of $\underline{I}_m$. The excited rotor "drags" the main field. The main field tries to brake the rotor and thereby the driving turbine. This explains the braking electromagnetic torque at generator operation. **The two dimensional flux plot** of Fig. 8.6 shows this state of operating: The braking torque can be seen by the tangential orientation of the flux lines in the air gap (**tangential magnetic pull**). At **motor operation**, the situation is reversed. Here, the excited rotor is "dragged" by the resultant air gap field; the torque M_e drives the rotor.

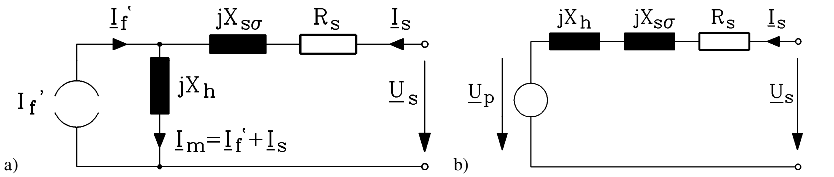

Fig. 8.4: Equivalent circuit per phase of a round-rotor synchronous machine: a) Current source equivalent circuit, where voltage drop of $\underline{I}'_f$ at jX_h gives $\underline{U}_p$, b) voltage source equivalent circuit

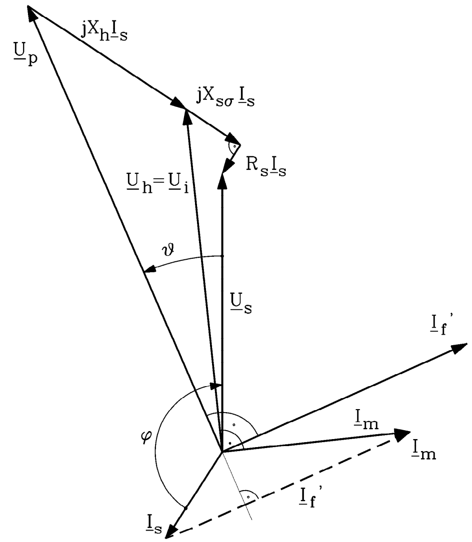

Fig. 8.5: Phasor diagram of a round-rotor machine. The chosen operating point corresponds to Fig. 8.2.

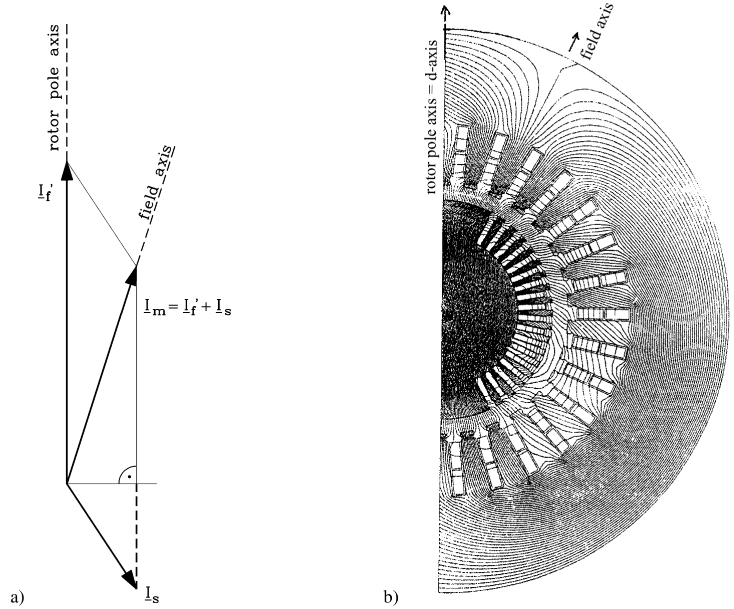

Fig. 8.6: Round-rotor synchronous machine: a) current phasor diagram, aligned to rotor pole axis, b) resultant numerically calculated magnetic flux lines of flux density B. **Two-pole turbo generator,** rated load 400 MVA,

21 kV, 11000 A, $\cos\varphi = 0.75$ overexcited, flux calculation with the finite element method, rotor main axis = direct axis, field axis = resultant main field.

8.3 Stator Equivalent Circuit of a Salient-Pole Machine

a) Magnetic Field and Flux Linkage:
In the contrary to the round-rotor machine, the air gap of a salient-pole machine is **not** constant. It is determined by the contour of the pole shoe and the gap between the poles, which causes a strong decrease of the magnetic air gap field. We assume that the rotor is not excited, but externally driven and rotates with synchronous speed n_{syn}. Only the stator current I_s flows. It excites the fundamental of the stator magnetic voltage $\hat{V}_s$ that rotates also with n_{syn}. If the maximum of the magnetic voltage distribution $V_s(x)$ occurs in ***d*-axis,** the air gap field $B_d(x)$ is **not sinusoidal**, even if the saturation of the iron is neglected, because the air gap $\delta(x)$ depends on the circumferential coordinate x.

$$B_d(x) = \mu_0 \frac{V_s(x)}{\delta(x)} \tag{8.24}$$

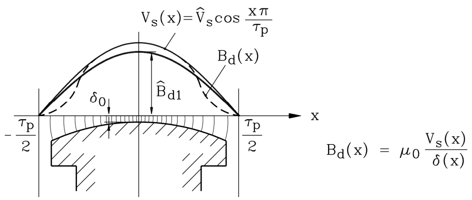

Fig. 8.7: The sinusoidally distributed stator magnetic voltage, oriented in *d*-axis, excites a non-sinusoidally distributed field $B_d(x)$ in the air gap, because the air gap is not constant along the circumference. The amplitude of the *FOURIER* fundamental of $B_d(x)$ has the amplitude $\hat{B}_{d1}$.

The amplitude $\hat{B}_{d1}$ of the fundamental $B_d(x)$ as determined by *FOURIER* analysis is smaller by the **field factor** c_d when compared with the amplitude $\hat{B}_s$ of a comparable round-rotor machine with constant air gap δ_0.

$$\hat{B}_s = \mu_0 \frac{\hat{V}_s}{\delta_0} \quad \text{(round-rotor machine)} \tag{8.25}$$

$$c_d = \hat{B}_{d1} / \hat{B}_s \quad \text{(salient-pole machine, } d\text{-axis)} \tag{8.26}$$

If the maximum of the magnetic voltage distribution $V_s(x)$ lies in the axis of the pole gap (***q*-axis, "quadrature axis"**) (Fig. 8.8), the air gap field distribution $B_q(x)$ is not sinusoidal either. The amplitude of the fundamental $\hat{B}_{q1}$ is **significantly smaller** than $\hat{B}_{d1}$, because of the decrease of the field in the inter-pole gap.

$$c_q = \hat{B}_{q1} / \hat{B}_s < c_d \quad \text{(salient-pole machine, quadrature axis)} \tag{8.27}$$

Result:

*The magnetic stator air gap field in the q-axis is smaller than in the d-axis for the same excitation $\hat{V}_s$. The "magnetic conductivity" (**reluctance**) of the path of the flux of the q-axis is by the relation c_q/c_d smaller than that of the d-axis **(= smaller q-axis reluctance).***

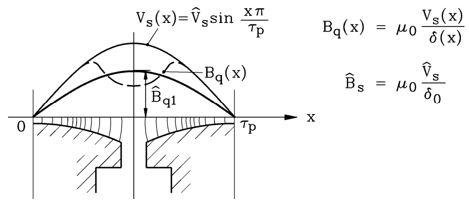

Fig. 8.8: The sinusoidal stator magnetic voltage excites a non-sinusoidal field distribution $B_q(x)$ in the axis of the inter-pole gap. The *FOURIER* fundamental of $B_q(x)$ has the amplitude $\hat{B}_{q1}$.

Fig. 8.9 shows the phasors $\underline{I}_s, \underline{I}'_f$ for overexcited generator operation in analogy to Fig. 8.5. Due to the different reluctance in *d*- and *q*-axis, the phasor $\underline{I}_s$ has to be decomposed into its components of *d*- and *q*-axis. The flux path of the *d*-axis is magnetised by $\underline{I}_{sd} + \underline{I}'_f$, the path of the *q*-axis by $\underline{I}_{sq}$. The *q*-flux $\underline{\Phi}_{qh}$ is much smaller than the *d*-flux $\underline{\Phi}_{dh}$, due to the smaller reluctance of the *q*-axis.

When compared with a round-rotor machine with the air gap δ_0, the magnetising inductance in the *d*-axis and the *q*-axis are by the factors c_d and c_q smaller:

$$\boxed{L_{dh} = c_d \cdot L_h} \qquad \boxed{L_{qh} = c_q \cdot L_h} \qquad L_h = \mu_0 (N_s k_{w,s})^2 \frac{2m_s}{\pi^2} \cdot \frac{l\tau_p}{p\delta_0} \tag{8.28}$$

b) Voltage Induction:
The stator flux linkage of the air gap field B_s, that is excited by the stator current I_s, depends on the relative position of the rotating field to the rotor. It is maximum for *d*-axis position and minimum for *q*-axis position. This is expressed by the corresponding inductances.

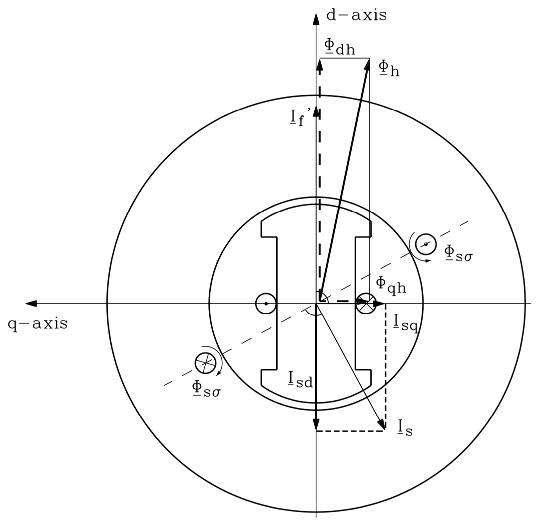

Fig. 8.9: Salient-pole machine: The *d*- and *q*-axis have different reluctance. Therefore, the phasor $\underline{I}_s$ has to be decomposed into the components of *d*- and *q*-axis to determine the total air gap flux Φ_h.

$$\Psi_{dh} = N_s \cdot k_{ws} \cdot \Phi_{dh} = L_{dh} \cdot I_{sd} \cdot \sqrt{2} \qquad (\Psi,\ \Phi\text{: peak values}) \tag{8.29}$$

$$\Psi_{qh} = N_s \cdot k_{ws} \cdot \Phi_{qh} = L_{qh} \cdot I_{sq} \cdot \sqrt{2} \tag{8.30}$$

The sinusoidal distribution of the stator magnetic voltage $\hat{V}_s$ is decomposed into two orthogonal sinusoidal functions with corresponding amplitudes $\hat{V}_{sd}, \hat{V}_{sq}$ for *d*- and *q*-axis, like the phasor $\underline{I}_s$ is decomposed into the components $\underline{I}_{sd}, \underline{I}_{sq}$ (Fig. 8.9). Due to the different **reluctances** of direct and quadrature axis, the magnetising flux (corresponding with phasor $\underline{I}_m$) is given for both axes separately:

$$d\text{-axis: } \underline{I}_{md} = \underline{I}_{sd} + \underline{I}'_f \qquad q\text{-axis: } \underline{I}_{mq} = \underline{I}_{sq} \tag{8.31}$$

The resulting stator and rotor m.m.f. is given by the magnetising current $\underline{I}_m$.

$$\underline{I}_m = \underline{I}_{md} + \underline{I}_{mq} \tag{8.32}$$

The flux linkage of the stator winding is:

$$\Psi_{dh} = L_{dh} I_{md} \cdot \sqrt{2} \qquad \Psi_{qh} = L_{qh} I_{mq} \cdot \sqrt{2} \tag{8.33}$$

The flux linkages oscillate sinusoidally with respect to time, thereby **inducing the internal voltage**

$$\underline{U}_h = j\omega_s \underline{\Psi}_h / \sqrt{2} = j\omega_s (L_{dh} \underline{I}_{md} + L_{qh} \underline{I}_{mq}) = \underline{U}_{qh} + \underline{U}_{dh} \tag{8.34}$$

with the components

$$\underline{U}_{qh} = j\omega_s L_{dh} (\underline{I}_{sd} + \underline{I}'_f) = j\omega_s L_{dh} \underline{I}_{sd} + \underline{U}_p \tag{8.35}$$

$$\underline{U}_{dh} = j\omega_s L_{qh} \underline{I}_{sq} \quad . \tag{8.36}$$

Considering the stator leakage inductance and the stator phase resistance, the **stator phase voltage equation** is obtained:

$$\underline{U}_s = R_s \underline{I}_s + j\omega_s L_{s\sigma} \underline{I}_s + j\omega_s L_{qh} \underline{I}_{sq} + j\omega_s L_{dh} \underline{I}_{sd} + \underline{U}_p \tag{8.37}$$

$\underline{I}_s$ is decomposed into its components of the *d*- and the *q*-axis:

$$\underline{U}_s = R_s \underline{I}_s + j\omega_s L_{s\sigma} (\underline{I}_{sd} + \underline{I}_{sq}) + j\omega_s (L_{qh} \underline{I}_{sq} + L_{dh} \underline{I}_{sd}) + \underline{U}_p$$

$$\boxed{\underline{U}_s = R_s \underline{I}_s + jX_d \underline{I}_{sd} + jX_q \underline{I}_{sq} + \underline{U}_p} \tag{8.38}$$

X_d is called **"synchronous reactance of the direct axis"**. X_q is called **"synchronous reactance of the quadrature axis"**, it is $X_d > X_q$.

$$\boxed{X_d = X_{s\sigma} + X_{dh} = \omega_s L_{s\sigma} + \omega_s L_{dh}},\ \boxed{X_q = X_{s\sigma} + X_{qh} = \omega_s L_{s\sigma} + \omega_s L_{qh}} \tag{8.39}$$

The round-rotor machine may be regarded as a "special case" of a salient-pole machine with $X_d = X_q$.

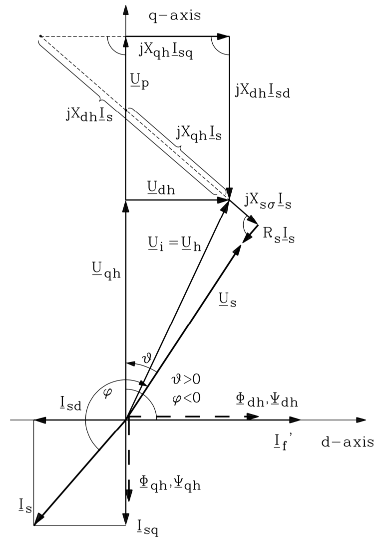

Fig. 8.10: Phasor diagram of a salient-pole synchronous machine: The chosen operating point corresponds to Fig. 8.9, but the figure is rotated by 90° to the right.

8.4 Performance of Line-Fed Round-Rotor Machines

8.4.1 Phasor Diagram for Different Operating Points at Line-Operation

The amplitude and the frequency of the line voltage is constant, independently of the load, because it is adjusted by controlled power plants (**"stiff" grid**). If a round-rotor machine is operated at such at stiff grid ($\underline{U}_s$ = const.), the following operating states can be obtained, as shown in Fig. 8.11.

Over-excitation (high synchronous generated voltage U_p) causes the stator current to be ahead of the stator voltage. The machine is a **capacitive load**, the reactive power is negative $Q < 0$, because the phase angle φ is negative. If the machine is externally driven, and the rotor is leading with respect to the rotating field (load angle $\vartheta > 0$), it works as a **generator**. At $\vartheta < 0$, the rotating field is leading the rotor, and the machine operates as a **motor**.

If the field current I_f is reduced, the internal voltage is reduced (**under-excitation**), the phase between the current and the fixed stator voltage changes. The phase angle φ becomes positive, the stator current lags behind the voltage, and the machine is an inductive load, similar to an induction machine ($Q > 0$).

In the following, the *OHM*ic stator phase resistance is neglected ($R_s \approx 0$), as – especially at large synchronous machines – it is much smaller than the synchronous reactance.

8.4.2 Phasor Diagram for Special Operating States

a) Generator at No-Load

The externally driven synchronous machine (Fig. 8.12a) is

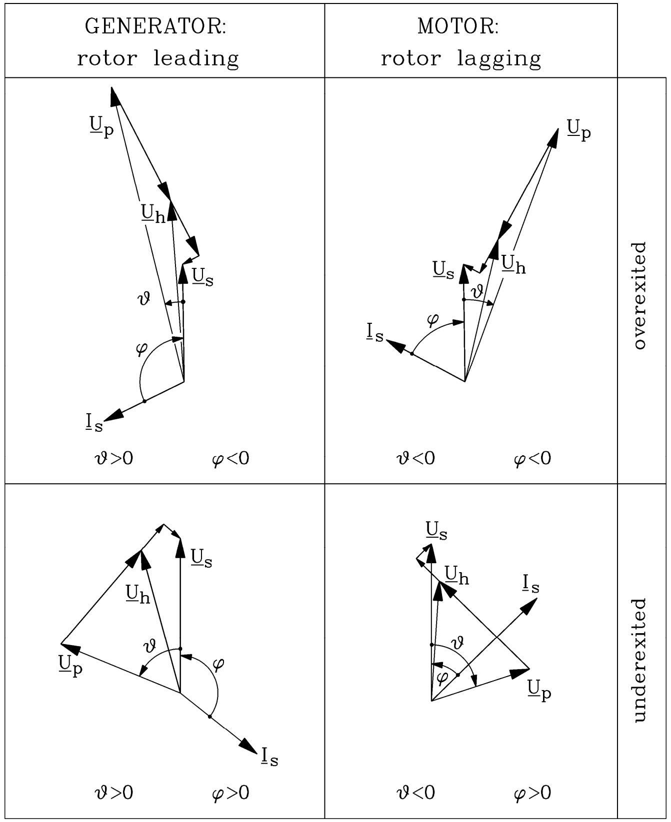

Fig. 8.11: Different states of operation of a round-rotor synchronous machine at fixed line voltage

(i) separated from the grid and the stator is at zero current. The machine is excited ($I_f > 0$). The stator phase voltage measured at the motor terminals equals the synchronous generated voltage U_p.

(ii) connected to the grid and excited so that the synchronous generated voltage U_p equals the line voltage. The corresponding no-load field current is called I_{f0}. Again, the stator does not consume any current. This situation is the condition for connection of an excited synchronous generator to the line (**"synchronisation"**): Amplitude and phase sequence (U, V, W) of internal and line voltage must be the same.

b) Phase Shifter Operation

Starting with generator no-load, the field current is increased (Fig. 8.12b) or reduced (Fig. 8.12c), so that the synchronous generated voltage and the terminal voltage remain in phase, but the first becomes either larger (case b) or smaller than the terminal voltage (case c). The machine operated as a capacitive (case b) or inductive load (case c). So, it acts either as a capacitor (case b) or as an inductor (case c) of variable size. The machine can be used to continuously adjust the **power factor** in the grid. As the load angle is zero, no active power, except for the losses, is converted inside the machine ($P = 0$).

c) Unexcited Line-Operation

Starting from underexcited operation (case c), the excitation is reduced down to zero (**non-excited operation**), and the synchronous generated voltage U_p becomes zero (Fig. 8.12d). Only the inductive current in the stator winding excites the air gap field, hence, it equals the **magnetising current**.

$$\underline{I}_s = \frac{\underline{U}_s}{jX_d} = \underline{I}_m \qquad (8.40)$$

d) Steady-State Short Circuit

At **steady-state short circuit** (Fig. 8.12e), the driven, not excited synchronous machine is directly shorted at the motor terminals and the field excitation in the rotor is increased, so that an internal voltage is induced in the stator winding. As U_s is zero, a steady-state short circuit current flows in the stator winding that is only limited by the synchronous reactance of the three phase winding and the small *OHM*ic stator resistance.

$$\underline{U}_s = \underline{U}_p + jX_d \underline{I}_s = 0 \quad \Rightarrow \quad \boxed{\underline{I}_{sk} = j\frac{\underline{U}_p}{X_d}} \quad (R_s \cong 0) \qquad (8.41)$$

The stator field that is excited by the **short circuit current** I_{sk} opposes to the rotor field. Only a small field amplitude remains in the air gap. It induces the **small internal voltage** U_h that equals the voltage drop of the stator short circuit current at the leakage reactance $X_{s\sigma}$ and the *OHM*ic stator resistance.

$$\underline{U}_h = -jX_{s\sigma}\underline{I}_{sk} \quad (R_s \cong 0) \qquad (8.42)$$

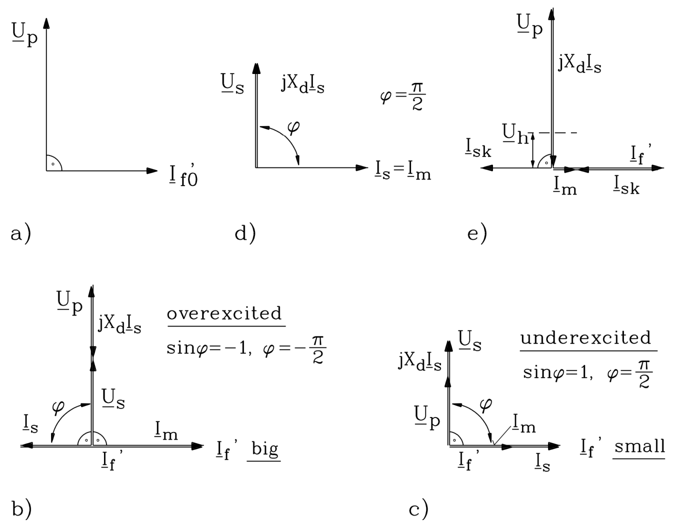

Fig. 8.12: Special states of operation of a round-rotor synchronous machine: a) generator no-load, b) phase shifter, overexcited, c) phase shifter, underexcited, d) line-operated, unexcited, e) steady-state short circuit

Example 8.4-1:

Braking of synchronous machines by short-circuit

After disconnection from the grid, synchronous machines may be brought to stand-still by a short circuit of the motor terminals that causes flow of a short circuit current. Together with the field of the rotor, the short circuit current creates a braking torque. The kinetic energy of the rotating rotor is converted into heat in the stator winding. The time to stand-still of the machine is much shorter than in the case of open-circuit run-out, where only friction losses are braking.

8.4.3 Torque-Load Angle Characteristic (at $R_s = 0$)

If $\underline{U}_s$ is constant, the active power that is converted in the synchronous machine P_e

$$P_e = m_s U_s I_s \cos\varphi = m_s \cdot \mathrm{Re}\left\{\underline{U}_s \underline{I}_s^*\right\} \qquad (8.43)$$

can be expressed as a function of the load angle ϑ. If U_s in defined onto the real axis, it is:

$$\underline{U}_p = U_p(\cos\vartheta + j\cdot\sin\vartheta) \qquad (8.44a)$$

The conjugate complex stator current phasor at $R_s = 0$ is obtained from the stator voltage equation:

$$\underline{I}_s = \frac{U_s - \underline{U}_p}{jX_d} \quad \Rightarrow \quad \underline{I}^*_s = \frac{U_s - \underline{U}^*_p}{-jX_d} \qquad (8.44b)$$

Combining (8.44b) and (8.43), the power as a function of ϑ is obtained:

$$P_e = m_s \cdot \mathrm{Re}\left\{U_s \cdot \frac{U_s - U_p(\cos\vartheta - j\cdot\sin\vartheta)}{-jX_d}\right\} = -m_s \frac{U_s U_p}{X_d}\sin\vartheta \qquad (8.45)$$

As the losses (R_s) are neglected, electric and mechanical power are identical (100 % efficiency). The electromagnetic torque of a round-rotor machine is:

$$\boxed{M_e = \frac{P_m}{\Omega_{syn}} = \frac{P_e}{\Omega_{syn}} = -\frac{m_s}{\Omega_{syn}} \cdot \frac{U_s U_p}{X_d}\sin\vartheta} \qquad (8.46)$$

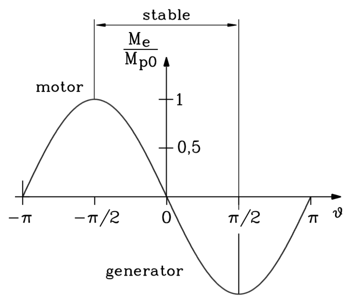

Fig. 8.13: Torque-load angle characteristic of a round-rotor synchronous machine

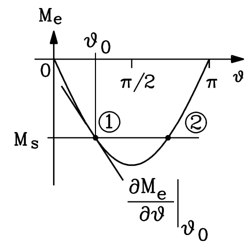

Fig. 8.14: Generator operation: operating point 1 is stable, operating point 2 is not stable. The limit of stability is at load angle $\pi/2$.

$$M_{e,\max} = M_s(\vartheta = \pm\frac{\pi}{2}) = \mp\frac{m_s}{\Omega_{syn}}\cdot\frac{U_s U_p}{X_d} = \mp M_{p0} \tag{8.47}$$

Result:
*The maximum torque occurs at $\vartheta = \pm 90°$ load angle (+ at generator, − at motor operation) (Fig. 8.13) and is called **"synchronous pull-out torque"** M_{p0}. It can by increased by an increase of the field excitation. A large synchronous reactance reduces the pull-out torque. If the load angle is positive, the electric power is negative, which is generator operation.*

8.4.4 Steady State Stability of a Synchronous Round-rotor Machine

Which combinations of torque and load angle allow for stable operation? It is assumed that a driving torque of a turbine M_s causes a load angle ϑ_0 at generator operation. Possible operating points are 1 and 2, given by the intersection of the $M_s(\vartheta)$ and $M_e(\vartheta)$ characteristics (Fig. 8.14).

$$M_e(\vartheta_0) = M_s(\vartheta_0) \tag{8.48}$$

The characteristic $M_e(\vartheta)$ is linearised by its tangent in the point ϑ_0:

$$M_e(\vartheta) \cong M_e(\vartheta_0) + \partial M_e/\partial\vartheta\cdot\Delta\vartheta \qquad \text{where} \qquad \Delta\vartheta = \vartheta - \vartheta_0 \tag{8.49}$$

The parameter c_ϑ describes the synchronous machine as an **equivalent torsional spring**. According to (8.50), because of the linear approximation by its tangent, the synchronous machine behaves like a linear torsional spring: An increase of the angle results in an increase of the torque.

$$c_\vartheta(\vartheta_0) = \frac{\partial M_e}{\partial\vartheta}\Big|_{\vartheta_0} \qquad \Leftrightarrow \qquad M_e = c_\vartheta\cdot\Delta\vartheta \tag{8.50}$$

A change of the load angle results in a change of speed $\Delta\Omega_m(t)$:

$$\frac{d\Delta\vartheta}{dt} = p\cdot\Delta\Omega_m \tag{8.51}$$

which is superimposed to the synchronous speed.

$$\Omega_m(t) = \Omega_{syn} + \Delta\Omega_m(t) \tag{8.52}$$

Combining (8.52) and NEWTON's law of motion, a linear differential equation of 2nd order with constant coefficients is obtained for the change of the load angle:

$$J\frac{d\Omega_m}{dt} = M_e(\vartheta) - M_s(\vartheta) = c_\vartheta\cdot\Delta\vartheta \qquad \Rightarrow \qquad J\frac{d\Omega_m}{dt} = J\frac{d\Delta\Omega_m}{dt} = c_\vartheta\cdot\Delta\vartheta$$

$$\boxed{J\frac{d^2\Delta\vartheta}{dt^2} - p\cdot c_\vartheta\cdot\Delta\vartheta = 0} \tag{8.53}$$

In the consumer reference frame, c_ϑ is negative for $|\vartheta| < \pi/2$ ($c_\vartheta = -|c_\vartheta|$) and positive for $|\vartheta| > \pi/2$ ($c_\vartheta = |c_\vartheta|$) (see Fig. 8.14).

a) $\underline{|\vartheta| < \pi/2}$:

$$\Delta\ddot{\vartheta} + (p\cdot|c_\vartheta|/J)\cdot\Delta\vartheta = 0 \quad \text{respectively} \quad \Delta\ddot{\vartheta} + \omega_e^2\Delta\vartheta = 0 \quad \Rightarrow \Delta\vartheta(t) \sim \sin(\omega_e t) \tag{8.54}$$

This is an **equation of an oscillation**. If the rotor is - e.g. by a perturbation of the driving torque – shortly displaced from the operating point, it oscillates around the operating point ϑ_0 against the "stiff" stator rotating field that is imposed by the grid. The **eigenfrequency** is:

$$f_e = \frac{\omega_e}{2\pi} = \frac{1}{2\pi}\sqrt{\frac{p|c_\vartheta|}{J}} \quad . \tag{8.55}$$

This oscillation is damped by the losses of the machine and often also by an additional damping cage (see Chapter 10). Hence, operating points with $|\vartheta| < \pi/2$ are **STABLE**.

b) $\underline{|\vartheta| > \pi/2}$:

$$\Delta\ddot{\vartheta} - (p\cdot|c_\vartheta|/J)\cdot\Delta\vartheta = 0 \quad \text{respectively} \quad \Delta\ddot{\vartheta} - \omega_e^2\Delta\vartheta = 0 \quad \Rightarrow \Delta\vartheta(t) \sim \sinh(\omega_e t) \tag{8.56}$$

The solution of this differential equation is a load angle deviation that increases exponentially: $\sinh(\omega_e t) = (e^{\omega_e t} - e^{-\omega_e t})/2 \approx e^{\omega_e t}/2$. Operating points with $|\vartheta| > \pi/2$ are **NOT STABLE**.

Result:
*Starting from no-load ($\vartheta = 0$), an increasing torque up to pull-out torque M_{p0} can be delivered by the machine. If the **pull-out angle** $\pm\pi/2$ is surpassed, the machine **pulls out of synchronism**. The rotor does not rotate synchronously with the stator rotating field, but it slips. Transmission of active power is no longer possible.*

8.5 Performance of Line-Fed Salient-Pole Machines

a) Torque Equation of a Salient-pole Machine, $R_s = 0$:

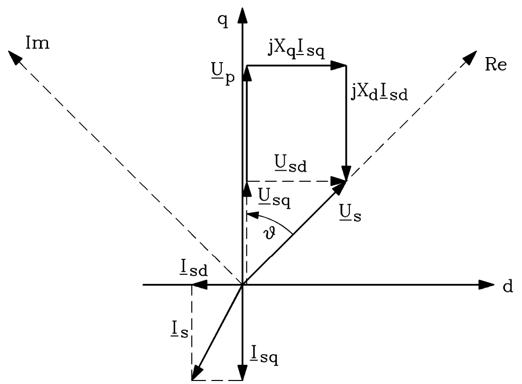

Fig. 8.15: Current and voltage phasor diagram of a salient-pole machine for an under-excited, generator operating point, $R_s = 0$ (The current is lagging).

In the phasor diagram of Fig. 8.15, $\underline{U}_s = U_s$ is put onto the real axis. Then, the synchronous generated voltage is a complex phasor:

$$\underline{U}_p = U_p \cdot e^{j\vartheta} \tag{8.57}$$

The components of U_s along the *d*- and *q*-axis are:

$$\underline{U}_{sq} = U_s \cdot \cos\vartheta \cdot e^{j\vartheta} = U_s \cdot \frac{e^{j\vartheta} + e^{-j\vartheta}}{2} \cdot e^{j\vartheta} \tag{8.58}$$

$$\underline{U}_{sd} = U_s \cdot \sin\vartheta \cdot (-j) \cdot e^{j\vartheta} = U_s \cdot \frac{e^{j\vartheta} - e^{-j\vartheta}}{2j} \cdot (-j) \cdot e^{j\vartheta} \tag{8.59}$$

The current components are obtained from the voltage equations ($R_s = 0$):

$$\underline{U}_{sq} = \underline{U}_p + jX_d \underline{I}_{sd} \quad \Rightarrow \quad \underline{I}_{sd} = \frac{\underline{U}_{sq} - \underline{U}_p}{jX_d} = \frac{je^{j\vartheta}}{X_d} \cdot \left(U_p - U_s \cdot \frac{e^{j\vartheta} + e^{-j\vartheta}}{2} \right) \tag{8.60}$$

$$\underline{U}_{sd} = jX_q \underline{I}_{sq} \quad \Rightarrow \quad \underline{I}_{sq} = \frac{\underline{U}_{sd}}{jX_q} = \frac{je^{j\vartheta}}{X_q} \cdot U_s \cdot \frac{e^{j\vartheta} - e^{-j\vartheta}}{2} \tag{8.61}$$

At a given terminal voltage $\underline{U}_s$ and back-e.m.f. $\underline{U}_p$, the current phasor $\underline{I}_s$ as a function of the load angle ϑ is obtained (Fig. 8.16).

$$\underline{I}_s = \underline{I}_{sd} + \underline{I}_{sq} = j\frac{U_p e^{j\vartheta}}{X_d} - j\frac{U_s}{2} \cdot \left(\frac{1}{X_d} + \frac{1}{X_q}\right) + j\frac{U_s}{2} \cdot e^{j2\vartheta} \cdot \left(\frac{1}{X_q} - \frac{1}{X_d}\right) \quad . \tag{8.62}$$

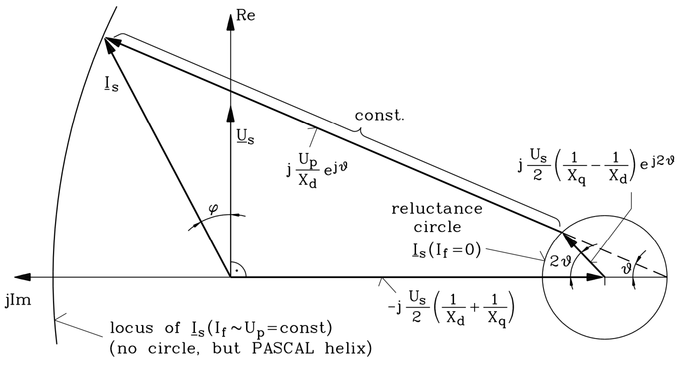

Fig. 8.16: Current locus diagram of a salient-pole machine at given stator and synchronous generated voltage as a function of the load angle

Using (8.62), the electromagnetic torque M_e is determined from the balance of power. As it is assumed that the machine has no losses, mechanical and electric power are identical. Large generators with 99% efficiency are close to this idealisation.

$$M_e = \frac{P_m}{\Omega_m} = \frac{P_m}{\Omega_{syn}} = \frac{P_e}{\Omega_{syn}} \tag{8.63}$$

$$M_e = \frac{1}{\Omega_{syn}} m_s U_s I_s \cos\varphi = \frac{p}{\omega_s} m_s \operatorname{Re}\left(\underline{U}_s \underline{I}_s{}^*\right) \qquad \Rightarrow$$

$$\boxed{M_e = -\frac{p \cdot m_s}{\omega_s}\left(\frac{U_s U_p}{X_d}\sin\vartheta + \frac{U_s^2}{2}\left(\frac{1}{X_q} - \frac{1}{X_d}\right)\sin 2\vartheta\right)} \tag{8.64}$$

The torque $M_e(\vartheta)$ (Fig. 8.17) consists of the **synchronous torque** (proportional to $\sin\vartheta$) due to the electrically excited rotor with a pull-out angle of 90° and an additionally occurring **reluctance torque** (proportional to $\sin 2\vartheta$) with a pull-out angle of 45°. Accordingly, the value of the steady state pull-out angle of the salient-pole machine is between 45° and 90°. The additionally occurring **reluctance torque** increases the overall torque of a salient-pole machine when compared with a round-rotor machine. Hence, the **stiffness** (**spring constant**), which is the increase of the torque characteristic as a function of the load angle, is larger than at a similar round-rotor machine.

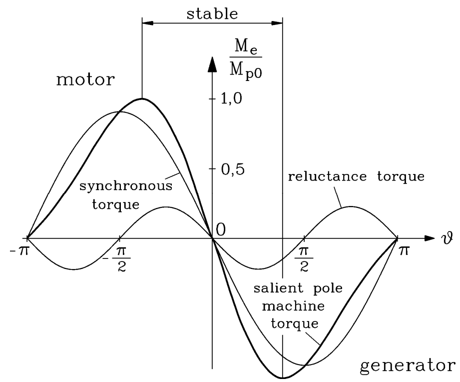

Fig. 8.17: Torque-load angle characteristic $M_e(\vartheta)$ of a salient-pole machine, referred to the value of the pull-out torque of a similar round-rotor machine M_{p0}

b) Reluctance Machine:

Even if the synchronous machine is unexcited ($I_f = 0 \rightarrow U_p = 0$), a torque – which is the **reluctance torque** – is generated, because of $X_d \neq X_q$. This torque is only caused by the different magnetic reluctance of *d*-axis and *q*-axis. The rotor has the tendency to orient its direct axis INTO the direction of the stator rotating field. This type of synchronous machine without winding in the rotor is called **reluctance machine** and is often used as a robust synchronous drive in the area of small rated powers (e.g. textile machines).

The rotor tries to move into the position where the field that is excited by the stator has to cross the minimum distance in the air gap. In Fig. 8.18 (1), the path across the air gap is minimum; the rotor has its preferred position at $\vartheta = 0°$ and does not produce any torque. In Fig. 8.18 (2), the rotor is moved from the preferential position (1) to $\vartheta = 45°$. It tries to return with maximum torque back to position (1), yielding generator "pull-out torque"). In Fig. 8.18 (4), the angle $\vartheta = -45°$ yields corresponding motor "pull-out torque". In Fig. 8.18 (3), the rotor is at unstable balance. The flux lines have to cross the path with the maximum length across the air gap. A small perturbation will bring the rotor back to position (1).

Result:

A reluctance machine operates with load angle $-45° < \vartheta < 0°$ *(motor) and* $0° < \vartheta < 45°$ *(generator).*

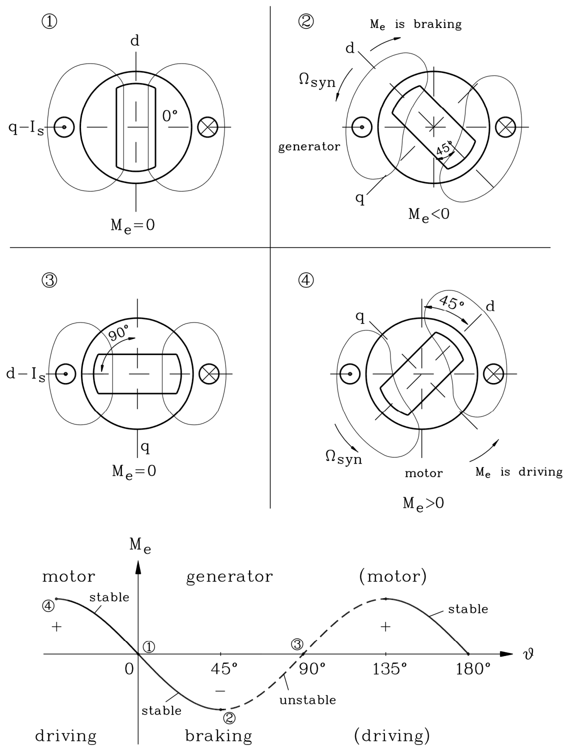

Fig. 8.18: Reluctance torque for different points of operation

8.6 Losses in Synchronous Machines

Large synchronous generators have a remarkable high efficiency η close to 1. Hence, the total losses P_d value only several percent of the rated power P_N.

Example 8.6-1:
Synchronous motor: P_N = 1 MW: η = 98%, percentage of losses P_d/P_N = 2%.
At machines with small power up to about 100 kW, the efficiency is usually smaller than 95 %. If the absorbed and delivered power is measured directly, and the efficiency and the losses are determined from that measurement, this is called **input-output test of efficiency** (European Standard EN60530/2).

$$\eta = \frac{P_{out}}{P_{in}} \qquad \Rightarrow \qquad P_d = P_{in} - P_{out} \tag{8.65}$$

For machines with efficiency larger than > 95 %, this method is not exact enough.

Example 8.6-2:

- efficiency of synchronous motor ($P_{out} = P_N$): η = 98%
- **measurement error** of measurement of P_{out}: F = 0.5%.
- total losses: $P_d = P_{in} - P_{out} \quad \Rightarrow \quad P_d / P_{out} = P_{in} / P_{out} - 1 = 1/\eta - 1 = 0.02$:

Measurement error at **determination of the losses** using the direct calculation of efficiency method: $F \cdot P_{out} = 0.005 \cdot P_{out} = 0.005 \cdot P_N = 0.005 \cdot (P_d / 0.02) = \underline{\underline{0.25 P_d}}$

- The total losses $P_d = 0.02 P_N$ are determined with 25% measurement error!

Therefore, the **efficiency is determined indirectly** from the measurement of the individual loss components $P_{d,i}$ according to the standard IEC34-2, respectively EN60530/2, because all (known) loss components can be measured with sufficient accuracy in this case.

$$\eta = \frac{P_{out}}{P_{out} + \sum_i P_{d,i}} \tag{8.66}$$

Three groups of **loss components** are distinguished (Table 8.1).

No load losses ($I_s = 0$)	- Iron losses: eddy current and hysteresis losses in the stator lamination (with frequency f_s) - additional no-load losses: e.g. eddy current losses in end plates - friction and ventilation losses
Load losses	- copper losses in the stator winding - additional stator load-losses e.g. eddy currents in stator winding, - additional rotor load losses e.g. eddy current on the rotor surface due to stator field harmonics etc.
Exciter losses	- copper losses in the field winding - losses in the excitation machine / the exciting converter and the slip rings etc., depending on the exciting system

Table 8.1: Loss components in synchronous machines

8.7 Synchronous Generators at Isolated Operation

If the synchronous machine is not line-operated, but as an isolated generator connected to a load (**"isolated operation"**), the **machine performance is quite different**. The speed controlled mechanical drive has to keep the speed constant to assure constant frequency. For example, the fuel injection pump of a variable speed diesel engine of a power stand-by unit or the steam of an industrial variable speed turbine may control speed. The terminal voltage of the generator must be adjusted via the field current.

Examples of Isolated Operation:
- claw pole synchronous machine as **dynamo** in motor vehicles (*Lundell* type generators),
- on-board generators of ships, planes (400 Hz) or railways
- diesel generator stations and wind turbines (islands, oasis, mountains)

At constant field current and speed, the **terminal voltage changes with the load**. The synchronous generator is considered as constant voltage source U_p with *OHMic*-inductive inner impedance (R_s and X_d), whereas the load e.g. may be *OHMic*-inductive or *OHMic*-capacitive (Fig. 8.19). The *OHMic*-inductive load is the most frequent type of load (e.g. induction motors, incandescent lights with reactors for ignition etc..). Capacitive load occurs e.g. if a synchronous generator supplies a overhead transmission line at no-load in case of "stand-by operation".

Applying *KIRCHHOFF*'s law to Fig. 8.19a, using Fig. 8.19b and the law of cosines, equation (8.67) is obtained.

$$U_p^2 = U_s^2 + (X_d I_s)^2 - 2U_s X_d I_s \cos\alpha \quad . \qquad (8.67)$$

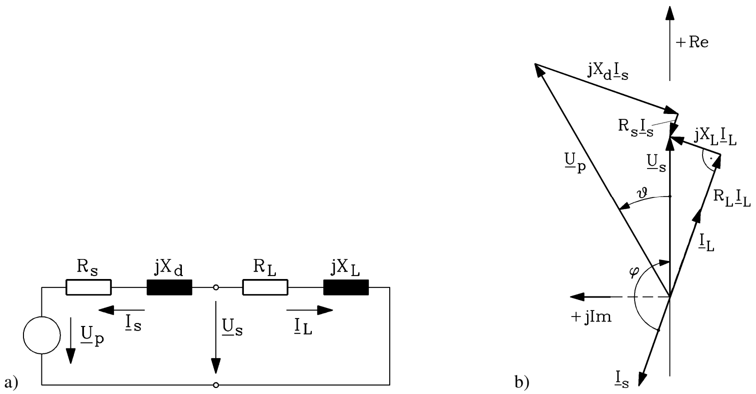

Fig. 8.19: Isolated operation of a round-rotor synchronous machine: a) equivalent circuit per phase at *OHM*ic-inductive load, b) corresponding phasor diagram

With $\alpha = 3\pi/2 - \varphi$ and the short circuit current $I_{sk} = U_p / X_d$, it is:

$$1 = \left(\frac{U_s}{U_p}\right)^2 + \left(\frac{I_s}{I_{sk}}\right)^2 + 2\frac{U_s}{U_p}\frac{I_s}{I_{sk}}\sin\varphi \qquad (8.68)$$

After introduction of the abbreviations $x = \frac{I_s}{I_{sk}}$, $y = \frac{U_s}{U_p}$, (8.68) becomes (8.69):

$$1 = x^2 + y^2 + 2xy\sin\varphi \quad . \qquad (8.69)$$

The coordinates are transformed from the *x*-*y*- into the ξ-η-system

$$x = (\xi - \eta)/\sqrt{2}\,, \quad y = (\xi + \eta)/\sqrt{2} \qquad (8.70)$$

to obtain the equation of an *ellipse* (8.71) from (8.69).

$$1 = \left(\frac{\xi}{a}\right)^2 + \left(\frac{\eta}{b}\right)^2 \qquad (8.71)$$

The main axes are: $a = \frac{1}{\sqrt{1+\sin\varphi}}$, $\quad b = \frac{1}{\sqrt{1-\sin\varphi}}$

Fig. 8.20 and Fig. 8.21 show these **ellipse sections** for the operating area of interest $U_s > 0$, $I_s > 0$, hence $x > 0$, $y > 0$.
At *OHM*ic-capacitive load, the phase angle is negative, hence $a > b$,
at *OHM*ic-inductive load, the phase angle is positive, hence $b > a$.
At 100 % reactive load, it is $\cos\varphi = 0$ and $\sin\varphi = 1$ (inductive load) respectively –1 (capacitive load). From equation (8.69), it is derived:

$y = -x + 1$ respectively $y = -x - 1$ at **inductive** load (8.72)

$y = x + 1$ respectively $y = x - 1$ at **capacitive** load (8.73)

As $y = -x - 1$ does not give positive voltage at positive current, it is not a solution for an actual state of operation.

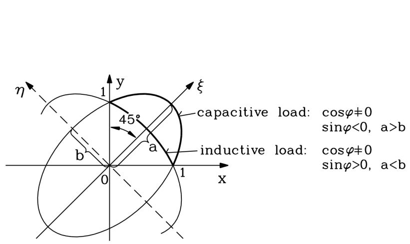

Fig. 8.20: Derivation of the external characteristic of a synchronous generator at isolated operation and constant excitation and speed, $R_s = 0$;
operation area $U_s > 0$, $I_s > 0 \Leftrightarrow x > 0,\ y > 0$.
*OHM*ic-capacitive load: $a > b$,
*OHM*ic-inductive load: $b > a$.

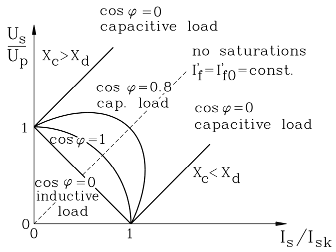

Fig. 8.21: External characteristic of a synchronous generator at isolated operation and constant excitation and speed, $R_s = 0$.

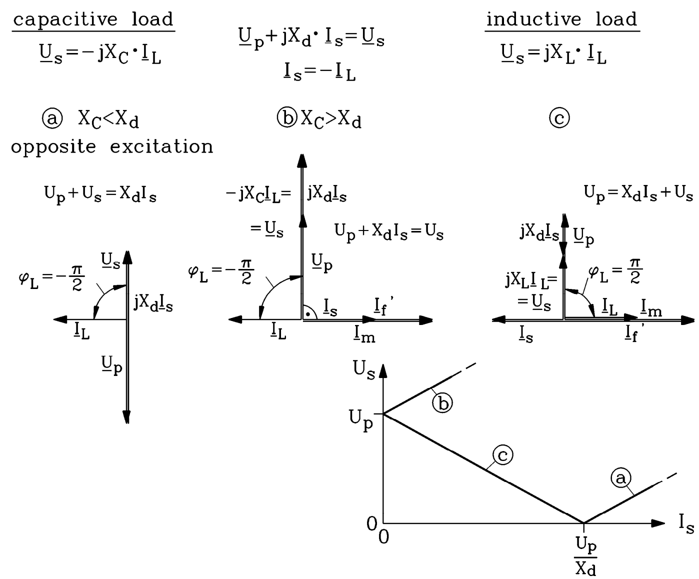

Fig. 8.22: Isolated operation at 100 % capacitive load (cases a, b) and 100 % inductive load (case c)

a) At **100 % capacitive load**, the terminal voltage increases $y = x - 1$, beginning at the **short circuit** point. Here, the load is bigger than the synchronous reactance $X_C < X_d$ (Fig. 8.22a). In reality, the increase of the voltage is limited by the increasing saturation of the iron.

b) At **100 % capacitive load**, the terminal voltage increases theoretically linearly ($y = x + 1$), beginning at the **no-load** voltage U_p. The load is smaller than the synchronous reactance $X_C > X_d$ (Fig. 8.22b).
c) At **100 % inductive load**, $y = -x + 1$, the terminal voltage decreases linearly with the load current I_s from no-load voltage U_p to short circuit point $U_s = 0$ (Fig. 8.22c).
d) At **100 % *OHM*ic load** ($a = b$), the characteristic is a quarter of a circle in the *x*-*y*-coordinate system.

It can be seen from the phasor diagrams 8.22, that the voltage increase at capacitive load occurs as a result of the increase of the magnetization current $\underline{I}_m$ as a sum of the field current $\underline{I}'_f$ and of the stator current $\underline{I}_s$. The voltage **IN**crease at load is known as ***FERRANTI* effect**. It is undesirable, because too high voltages may endanger the equipment.

Remark:
In Fig. 8.22a, COUNTER-excitation (negative excitation) occurs; back-e.m.f. and terminal voltage are phase-shifted by 180°. However, a 180° load angle does **not** lead to instability, because the stator voltage and hence the stator rotating field are not externally determined in the case of isolated operation, but can adjust freely according to the load. Therefore, NO torque characteristic as in Fig. 8.13 with a pronounced pull-out behaviour and **no oscillation of the rotor** against the stator rotating field as in Fig. 8.14 occurs.

Example 8.7-1:
An unexcited synchronous generator of a power plant is externally driven ($I_f = 0$) and an overhead line with open terminals and $X_C = 1/(\omega C)$ impedance is connected to its terminals ("stand-by"). A small rotor voltage U_{pR} is induced in the stator winding due to the iron remanence field B_R of the rotor poles. This voltage causes a small capacitive loading current I_L, that increases the voltage according to Fig. 8.22b. At open terminals of the overhead line, a considerable voltage occurs, although the field winding of the synchronous machine is at zero current (**"self excitation of synchronous machine"**).

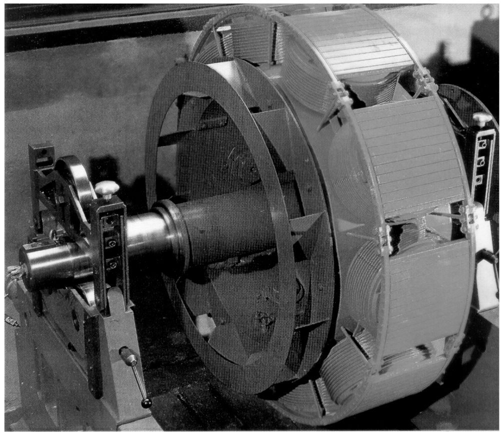

Fig. 8.23: 8-pole salient-pole rotor with damper (Chapter 9) and radial fan during balancing